

Improving the Grid Power Quality Using Virtual Synchronous Machines

Yong Chen¹, Ralf Hesse², Dirk Turschner³ and Hans-Peter Beck⁴

Institute of Electrical Power Engineering, Clausthal University of Technology, Germany

¹yong.chen@tu-clausthal.de, ²email@ieh.w.de, ³dirk.turschner@tu-clausthal.de, ⁴mendt@iee.tu-clausthal.de

Abstract – This paper presents the improvement of power quality and grid stability for distributed generation using the virtual synchronous machine (VISMA) which embodies a hysteresis controlled three phase inverter with a synchronous machine model on an embedded control computer to calculate the reference currents. Currently the conventional grid-connected inverters are predominantly designed to transmit electrical energy to the grid discounting the maintenance of frequency and voltage and also its transient stability. However, the VISMA is able to regulate both the active and reactive power separately and bidirectionally by setting the virtual torque and virtual excitation to meet the power system requirements. Furthermore, a virtual rotating mass is implemented in the VISMA in order to increase the inertia in the grid and improve the transient frequency stability in analogy to the conventional synchronous generator. Additionally, the virtual damping of the VISMA can reduce the frequency and power oscillation in the grid. All these properties mentioned above have been verified in simulations and measurements in an experimental micro grid.

Index terms - virtual synchronous machine (VISMA), virtual rotating mass, virtual damping, inverter, grid stability, distributed generation.

I. INTRODUCTION

The increasing integration of distributed generation (DG) sources is accompanied by problems with primary energy resources and policy issues such as economic efficiency, environmental protection and energy security [1].

DG technologies include photovoltaic, wind turbines, fuel cells, small and micro sized turbine sets, stirling engine based generators and combustion engine driven generators [2]. Some of these DG technologies such as photovoltaic or fuel cells produce direct current and must be connected to the grid via inverters. The wind turbines can provide alternating current, however, due to the variable wind speed, the inverter has to handle the generator and grid frequency gap. One of the disadvantages of such power electronic interfaces is the lack of synthetic inertia, which energetically corresponds to the electrical short-time storage in the inverter to inhibit frequency strokes in the grid caused by transient power unbalances or partial grid shedding. The computation of the rotating generator mass on the control computer increases the transient grid frequency stability. Furthermore, the conventional inverter concept is designed to transmit a maximum energy harvest into the grid neglecting the power quality. This may lead to disturbances of the voltage profile: due to the bidirectional power flows and the insufficient

control, the voltage in the whole grid may fluctuate [3]. Hence, a reliable voltage control method is required.

Generally, a few small-size DG units will not influence the safe operation of the power network in the presence of large centralized power stations and so their attendance can be neglected. But with a larger numbers of DG units with higher capacities, the overall dynamics of power systems are significantly affected [4].

The study of variable DG technologies shows an increase of the maximum frequency deviation if the output power of the DG units raises [3]. In addition, the synchronous generator has a larger effect on the voltage stability because of its capability of reactive power provision [5]. Moreover, the synchronous generators can operate self-organizing highly parallel, reliable and stable.

Because of these advantages it is appropriate that DG units with inverter should operate as synchronous generators to improve the power quality in distributed grids. Based on this approach, some further control strategies were developed such as *Droop Control* [6], *Virtual Synchronous Generator* [7] and *Synchronverter* [8]. These concepts render only fragments of the static and dynamic property compound of the synchronous machine.

In comparison, the VISMA concept contains the entire static and dynamic properties. This paper presents these properties, the VISMA hardware structure and the improvement of the power quality. Firstly, the basic principle of the VISMA is illustrated in section 2. Secondly, the static and dynamic properties are shown as simulation results in section 3. Subsequently, in section 4 the experimental micro grid in the laboratory is introduced and the measurement results are demonstrated.

II. PRINCIPLE OF VISMA

A. Control strategy

The VISMA concept aims to set up the static and dynamic performance of the electromechanical synchronous machine on a three phase hysteresis controlled inverter with battery storage so that a DG unit with grid inverter interface is going to operate like a conventional synchronous machine. Fig. 1 shows the basic structure of the VISMA.

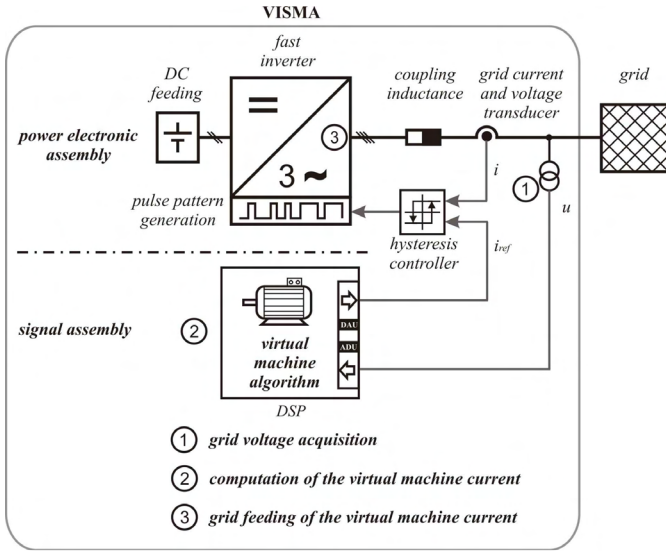


Fig 1: Basic structure of the VISMA.

A complete VISMA functional chain contains three sub-processes. It starts with the real-time measurement of the grid voltage (1) to feed the virtual synchronous machine algorithm (2) on the process computer which performs the mathematical model of an electromechanical synchronous machine under real-time condition. The results are the stator currents of the virtual synchronous machine, present as process variables. To complete the cycle, the calculated currents have to take effect to the grid. For this purpose the fast hysteresis controlled inverter (3) carries over the reference current signals to drive these currents to the grid immediately.

The performance of the virtual synchronous machine is adjustable by modification of the VISMA model parameters at the computer any time while the process is running. The variation of the parameters directly affects the calculated stator currents and thus the operation of the inverter. Aside from higher frequency noise due to inverter's switch activity, from the grid's point of view there is no difference between the electrical appearance of an electromechanical or a virtual synchronous machine.

B. Calculating the reference currents

As mentioned above, the VISMA is based on a fast current control method, therefore, VISMA's performance essentially depends on the reference currents, which are calculated with the assistance of a synchronous machine model and include all information about static and dynamic properties. Hence, the precision of modeling a synchronous machine influences the performance of the VISMA directly.

In this paper a three-phase model of the synchronous machine is used to calculate the reference currents. The three-phase model reproduces the stator circuit of a synchronous machine and the mechanical subsystem, which provides the features virtual rotating mass and virtual damping according to the electromechanical power balance. Instead of a field circuit, the pole wheel induction voltage in the stator is

considered and the damping feature is directly incorporated in the mechanical subsystem, see Fig. 2.

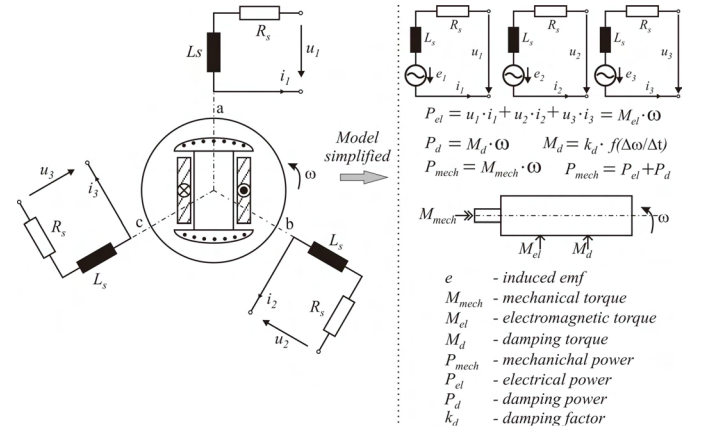


Fig 2: Simplified synchronous machine model.

The stator circuit is described by:

$$e_1 - u_1 = i_1 \cdot R_s + L_s \cdot \frac{di_1}{dt} \quad (1)$$

$$e_2 - u_2 = i_2 \cdot R_s + L_s \cdot \frac{di_2}{dt} \quad (2)$$

$$e_3 - u_3 = i_3 \cdot R_s + L_s \cdot \frac{di_3}{dt} \quad (3)$$

$$\vec{e} - \vec{u}_{grid} = \vec{i}_{ref} \cdot R_s + L_s \cdot \frac{d\vec{i}_{ref}}{dt} \quad (4)$$

where $\vec{e} = [e_1 \ e_2 \ e_3]^T$ is the induced EMF (electromotive force) in the stator windings, $\vec{u}_{grid} = [u_1 \ u_2 \ u_3]^T$ embodies the grid voltages at the point of common coupling (PCC), R_s is the stator resistance and L_s the stator inductance. The reference currents $\vec{i}_{ref} = [i_1 \ i_2 \ i_3]^T$ can be calculated in the Laplace domain via

$$\vec{i}_{ref}(s) = (\vec{e}(s) - \vec{u}_{grid}(s)) / (R_s + L_s \cdot s) \quad (5)$$

To simplify the interaction between stator and rotor, the electromechanical power balance is introduced, see Fig. 2.

The following equations regard the rotor dynamic:

$$M_{mech} - M_{el} = \frac{1}{J} \cdot \frac{d\omega}{dt} + k_d \cdot f(s) \cdot \frac{d\omega}{dt} \quad (6)$$

$$M_{el} = \frac{P_{el}}{\omega} \quad (7)$$

$$\theta = \int \omega \cdot dt \quad (8)$$

J is the moment of inertia, k_d is the mechanical damping factor, $f(s)$ is the phase compensation term, ω the angular velocity, θ is the angle of rotation, M_{el} and M_{mech} are the electrical and mechanical torque. The phase compensation term ensures that the virtual damping force counteracts any oscillating movement of the rotor in opposite phase.

Despite of simplifying the excitation winding, the induced EMF is given by an adjustable amplitude E_p and the rotation angle θ , i.e.:

(9)

The block diagram illustrates the control system for a Permanent Magnet Synchronous Motor (PMSM). The system includes a reference current \bar{i}_{ref} and a feedback loop. The reference current \bar{i}_{ref} is compared with the actual current \bar{i} to produce the current error \bar{e} . This error is integrated and then multiplied by the current feedback gain R_s to produce the reference current \bar{i}_{ref} . The reference current \bar{i}_{ref} is compared with the actual current \bar{i} to produce the current error \bar{e} . This error is integrated and then multiplied by the current feedback gain R_s to produce the reference current \bar{i}_{ref} . The reference current \bar{i}_{ref} is compared with the actual current \bar{i} to produce the current error \bar{e} . This error is integrated and then multiplied by the current feedback gain R_s to produce the reference current \bar{i}_{ref} .

Fig. 3: Block diagram of the three-phase model.

The simplifications of the three-phase model result to a lack of the transient and sub-transient stator current components. However, implementing a parallel secondary machine with the same structure but more dynamic stator parameters and joining together the instantaneous stator current signals of both machines, the features of transient and sub-transient stator currents are facile extendable. In this way, the transient machine behavior could be set almost freely [9].

III. PROPERTIES OF THE VISMA

In this section, the static and dynamic properties of the VISMA are investigated and shown in simulation results.

A. Active and reactive power Setting

In the centralized power plant, the supply of active power can be adjusted by setting the mechanical torque of the synchronous generator whereas the reactive power can be regulated by setting the current in the excitation winding. VISMA has equivalent controlling elements, the model parameters virtual torque M_{mech} and virtual exciting E_p as illustrated in Fig. 3.

Fig. 5 shows a simulation result of an active power response P_{VISMA} while the virtual torque M_{mech} springs from 0 to $5Nm$. Once the virtual torque is set, an active current flows immediately, which results an active power flow consequently. The current and power oscillation after the torque step is caused by the mechanical rotor inertia which also occurs in synchronous generators in power plants.

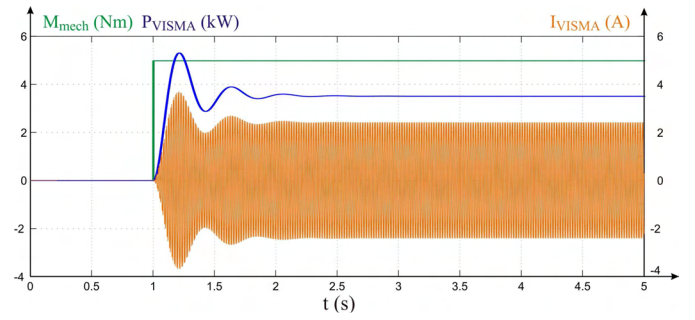


Fig. 5: Generating active power by setting the virtual torque.

In the next simulation shown in Fig. 6, the virtual torque is slowly changed, so that no power oscillations occur. The positive torque leads to a motor operation of the VISMA, which means the electrical energy flows from the grid into the battery so that the surplus energy in the grid can be stored in the battery. This operation mode can only be achieved with the VISMA, compared to conventional power plants with synchronous generators. Conversely with a negative torque, the battery will be discharged and the grid will be supported by the VISMA.

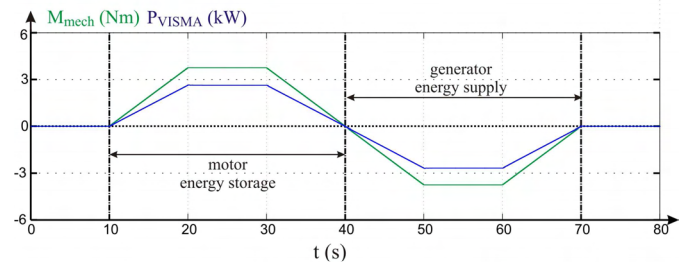


Fig. 6: Bidirectional active power setting.

The simulation results in Fig. 7 prove that the reactive power $Q_{VISM A}$ changes proportionally to the variation of the virtual excitation ΔE_p . Similar to the active power setting, VISMA can also feed the reactive i.e. inductive and capacitive power, into the grid bidirectionally. This property is important for the grid voltage maintenance and as evidenced by measurements shown in the next section.

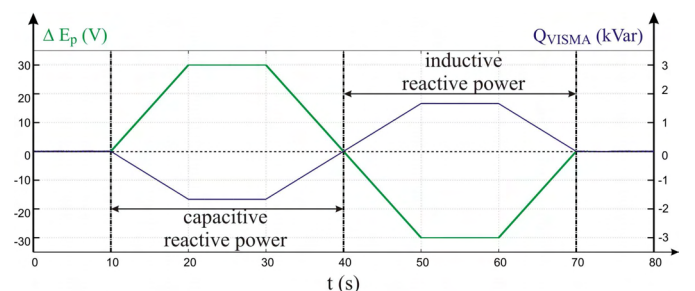


Fig. 7: Bidirectional reactive power setting.

B. virtual rotating mass

In conventional power systems, there is a close relation between the grid frequency and the rotor speed of all synchronous generators. Because of the moment of inertia,

the rotor speed and thus the grid frequency cannot change suddenly while load activity. Therefore, the transient frequency stability will be improved by increasing the rotating mass in the grid. This feature of synchronous machines is also inherited in the VISMA concept implementing a *virtual rotating mass* J regarded in equation (6).

In order to investigate the dynamic effect of the virtual rotating mass, different amounts of it are chosen and the power reaction of the VISMA is recorded while a grid frequency drop of $\Delta f_{grid} = 0.5\text{Hz}$ caused by load activation. The simulation results are presented in Fig. 8.

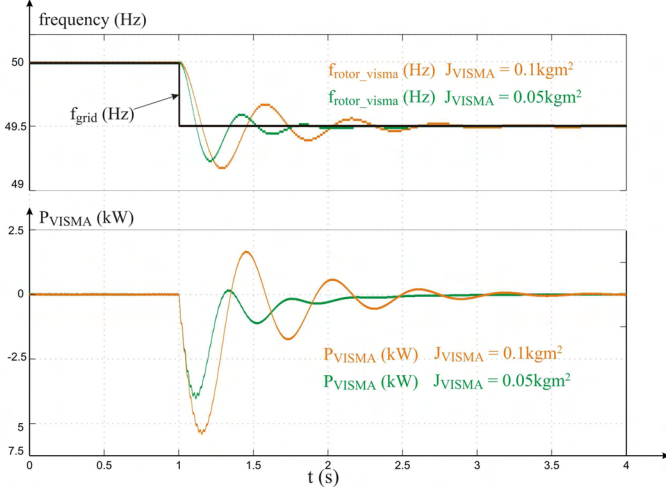


Fig. 8: Effect of the virtual mass.

It can be clearly seen that the VISMA provides active grid power immediately as the grid frequency drops. Comparing the power reactions with $J_{VISMA} = 0.05\text{kgm}^2$ and $J_{VISMA} = 0.1\text{kgm}^2$, it can also be observed that a VISMA with a larger virtual mass will provide more active power into grid. The virtual rotating mass can be freely adjusted in the VISMA model as against conventional synchronous machines.

C. Virtual damping

The Fig. 8 indicates that the amplitude of the observed power oscillation depends on the amount of the virtual mass. This oscillation can be reduced by the virtual damping, the second important dynamic property of VISMA that improves the power system stability. To illustrate this effect, the simulations regards two different amounts of the damping factor k_d in the VISMA model. Fig. 9 shows the frequency step response of a VISMA with various damping setting.

IV. EXPERIMENTAL RESULTS

To verify the simulation results, an experimental micro grid was set up, which consists of two asynchronous-synchronous

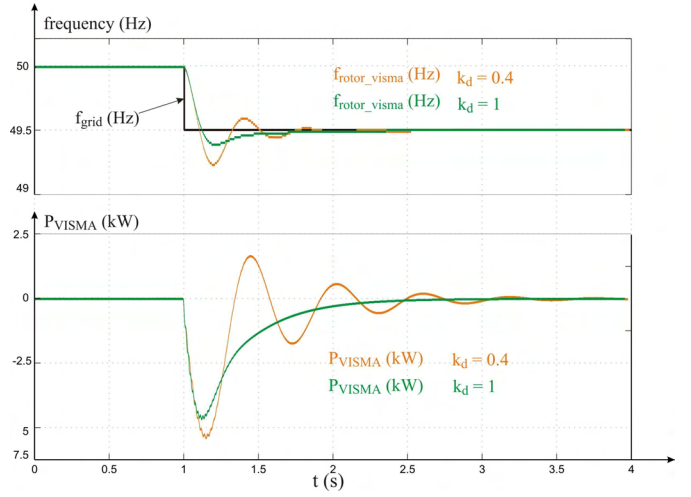


Fig. 9: Effect of the virtual damping.

-machine-sets (ASM-SM-sets) with a nominal power of 15kW each and two VISMA systems with one battery group for each system featuring 5kW nominal power. Fig. 10 shows the block diagram of the experimental micro grid.

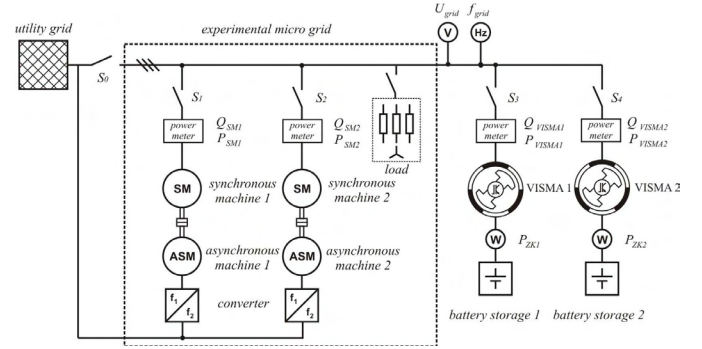


Fig. 10: VISMA experimental micro grid.

The two ASM-SM-sets represent conventional controlled power plants so it is possible to provide typical frequency and voltage changes in the grid caused by load activity. With the electromechanical synchronous machines, the experimental grid can be run in island mode. By switching S_0 , a parallel operation to the utility grid can also be achieved. Instead of a complete generator and storage system, only battery units are provided for the VISMA DC-link, which is otherwise fed by photovoltaic, wind generators, fuel cells and CHPs (combined heat and power). Despite this simplification all relevant operating conditions, particularly the bidirectional energy flow on the DC side, can be observed. The installed local storages of the VISMA systems can also serve as charge station for electro mobiles.

A. Active and reactive power setting

In this case, one of the VISMA systems is connected to the utility grid (Fig. 11). The virtual torque and the virtual excitation of the VISMA are set separately and slowly enough so that almost no oscillations occur in the grid.

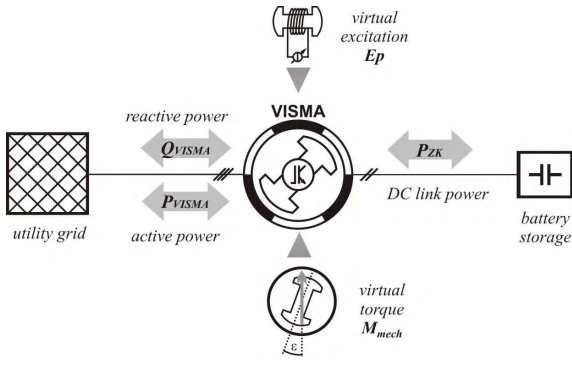


Fig. 11: Measurement of the power flows by setting virtual torque and excitation.

Fig. 12 shows the track of VISMA active power (blue), corresponding power in the DC-link (light red) and the reactive power (red), that follows the active power mutually, depending on the arbitrary chosen shape of the virtual torque M_{mech} . It is obvious that the active power follows the virtual torque linearly. Meanwhile, the reactive power changes appreciably, because of the coupling between the active and reactive power which can also be observed on conventional synchronous machines.

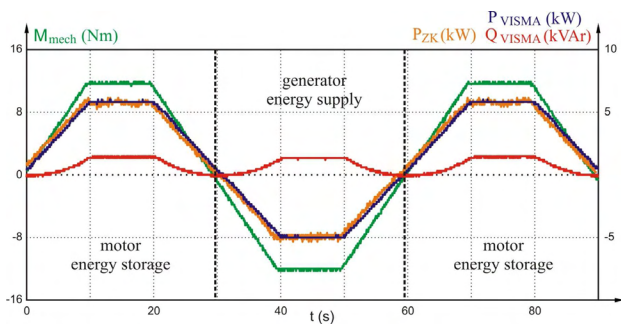


Fig. 12: Investigation of the active, reactive and DC-link power in dependence of the virtual torque in VISMA.

In the subsequent experiment, the virtual excitation E_p is also arbitrary changed rendered with the green curve shown in Fig. 13 in order to study the phase shifter operation. The inductive and capacitive reactive power varies proportionally to the changes of the virtual excitation.

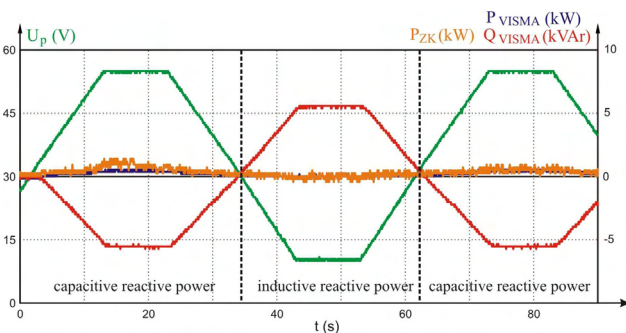


Fig. 13: Investigation of the active, reactive and DC-Link power in dependence of the virtual excitation in VISMA.

B. controlling active and reactive power like power plants

As the electromechanical synchronous generator, VISMA can be equipped with frequency and voltage control loops to meet the grid power demand automatically. The control structure is represented in Fig. 14.

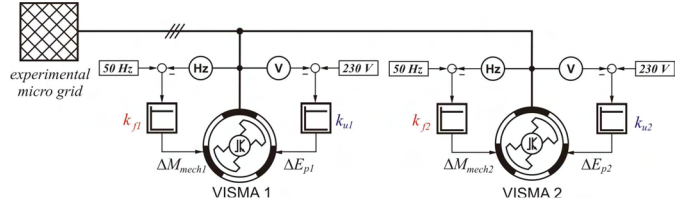


Fig. 14: Dynamically setting the power flows of VISMA by frequency and voltage control.

In Fig. 15, the measurement results of the frequency control are recorded. The experiment starts with a nominal frequency deviation of $\Delta f_{grid} = 1\text{Hz}$ in the experimental micro grid with slower tuned ASM-SM-sets. By activating the frequency control of VISMA 1 ($t = 20\text{s}$), it provides immediately active power for the grid and counteracts the frequency deviation. At this time, VISMA 2 only supports transient active power because of its virtual rotating mass. If the frequency control of VISMA 2 is also activated ($t = 40\text{s}$), the deviation of the grid frequency becomes smaller once again. Choosing the same P-value for both proportional frequency controllers, the grid power contribution of the VISMA is auto-balanced.

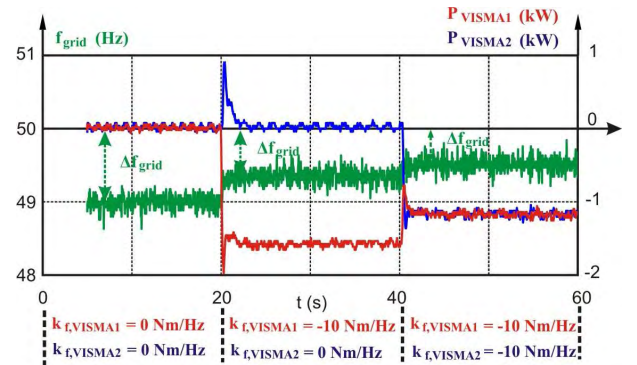


Fig. 15: Frequency control and active power regulation.

In the second part of the experiment, the voltage controller is enabled while the frequency controller is disabled. At the beginning, the deviation of the nominal grid voltage is set to $\Delta U_{grid} = 10\text{V}$ with lower tuned SM excitation voltages. In the time range $t = 0 \dots 20\text{s}$, the two VISMA systems naturally supply reactive power in spite of the initially inactivated voltage controller because of the difference between U_{grid} and initial value E_p of the VISMA model. However, it is not enough to compensate the imbalance of reactive power in the grid. At $t = 20\text{s}$ the voltage controller of VISMA 1 is activated and then the grid voltage deviation becomes smaller to $\Delta U_{grid} = 5\text{V}$. By activating the voltage control of both VISMA systems ($t =$

40s), the voltage deviation decreases to $\Delta U_{grid} = 3V$. To widely compensate the voltage deviation, the controller gain k_u should be further increased. The difference between the power flows of both VISMA systems although the same k_u is caused by inaccuracies in the voltage measuring transformer system. Usually the reactive power response of the VISMA is also auto-balanced.

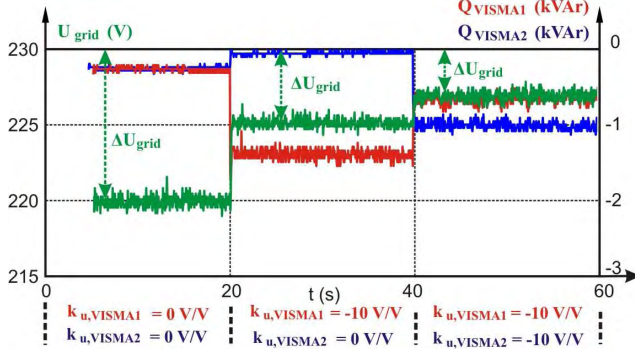


Fig. 16: Voltage control and reactive power regulation.

C. Frequency support of virtual rotating mass

As presented in section III, the virtual rotating mass of the VISMA can improve the transient frequency stability of the power system. This dynamic property can be proved while activating a load in the experimental micro grid (Fig. 10). To illustrate the relationship between the frequency backing and the virtual rotating mass, three experiment cases are carried out, i.e. activated load without VISMA, with one and with two VISMA. The measurement results are documented in Fig. 17. It can be clearly seen that the experimental micro grid without VISMA shows the maximum frequency drop when switching on the load. With the support of the VISMA, the frequency drops slower and the deviation is decreased. The grid frequency stiffness increases with the number of activated VISMA systems because of the growing entire rotating mass in the grid.

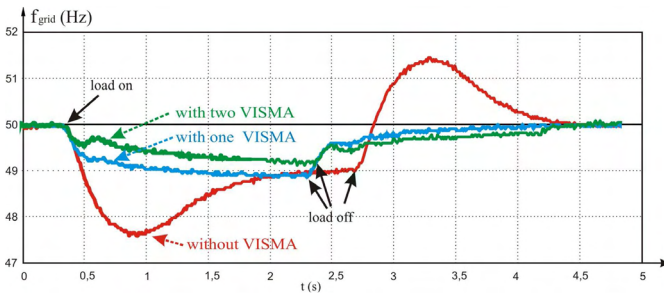


Fig. 17: The virtual rotating mass of VISMA counteracts the frequency drop.

D. Dynamic effects of the virtual damping

In order to investigate the damping effects of the VISMA, a frequency oscillation in the experimental grid is excited by periodically switching a load. At first the damping factor of the VISMA is set to $k_d = 0.1$. In this case, a frequency oscillation with an amplitude of $\Delta f_{grid} = 1.9Hz$ can be

observed (Fig. 18). If the damping factor is increased to $k_d = 0.5$, a reduction of the amplitude from 1.9Hz to 1.2Hz is detectable. The virtual mass remains unchanged.

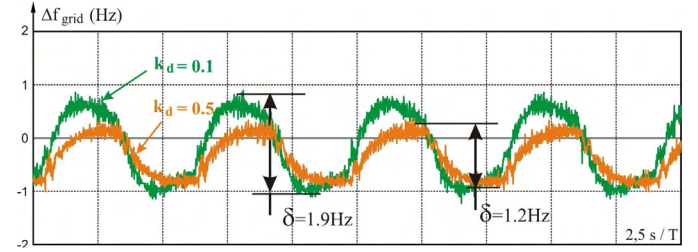


Fig. 18: The virtual damping of VISMA reduces the frequency oscillation.

V. CONCLUSIONS

This paper introduces the VISMA concept to upgrade grid feeding inverters with synchronous machine behavior to improve the power quality and stability of the grid.

The investigations of the VISMA's static and dynamic properties via simulation and experimental measurements confirm its predicted grid behavior.

The VISMA approach offers a solution for the self organizing decentralize feeder of renewable energy without system intercommunication. With the same configuration of the local frequency and voltage controllers, all VISMA meets the grid power demand auto-balanced, so it is easy to spread solar surplus energy over the whole grid. The short-time frequency stiffness of the grid grows with the number of active VISMA and grid oscillations will be damped cooperatively.

REFERENCES

- [1] International Energy Agency IEA, "Distributed Generation in Liberalised Electricity Markets", Paris, 2002.
- [2] P.P. Barker, R.W. De Mello, "Determining the impact of distributed generation on power systems. I. Radial distribution systems", *IEEE PESS 2000*, pages 1645 - 1656 vol. 3, USA, ISBN 0-7803-6420-1.
- [3] Ahmed M. Azmy, I. Erlich, "Impact of Distributed Generation on the Stability of Electrical Power Systems", in *Proc. IEEE PES*, 2005.
- [4] J. G. Sloopweg, W. L. Kling, "Impacts of distributed generation on power system transient stability", *Power Engineering Society Summer Meeting, 2002 IEEE*, Vol.: 2, 21-25 July 2002, Pages:862 - 867 vol.2
- [5] J. Driesen, R. Belmans, "Distributed Generation: Challenges and Possible Solutions", in *Proc. IEEE PES*, 2006.
- [6] A. Engler, N. Soutanis, "Droop control in LV-grids", in *Proc. IEEE FPS*, 2005, Amsterdam.
- [7] J. Driesen, K. Visscher, "Virtual synchronous generators", in *Proc. IEEE PES 2008*, pages 1-3.
- [8] Q.C. Zhong, G. Weiss, "Synchronverter: Inverters that Mimic Synchronous Generators", *IEEE Transactions, Industrial Electronics*, issue 99, 2010.
- [9] Y. Chen, R. Hesse, D. Turschner, H.P. Beck, "Dynamic Properties of Virtual Synchronous Machine (VISMA)", in *Proc. ICREPQ*, 2011, Spain.